Gyromagnetic ratios in ^{164}Dy and ^{168}Er

C. E. Doran*
School of Physics, University of Melbourne, Parkville, Victoria, Australia 3052

A. E. Stuchbery
Department of Nuclear Physics, Research School of Physical Sciences, Australian National University, P.O. Box 4, Canberra, Australia 2601

H. H. Bolotin, A. P. Byrne,† and G. J. Lampard
School of Physics, University of Melbourne, Parkville, Victoria, Australia 3052
(Received 17 July 1989)

Gyromagnetic ratios of levels up to 10^+ in the ground-state bands and of the 2^+ states in the γ bands of ^{164}Dy and ^{168}Er were measured by the perturbed angular correlation technique utilizing the transient hyperfine field acting at the nuclei of these ions as they swiftly traversed thin polarized Fe foils. The experimental g factors, together with the results of earlier similar studies for ^{166}Er, are discussed and compared with several theoretical predictions.

I. INTRODUCTION

By virtue of the relatively large intrinsic magnetic moments of individual nucleons compared with the collective nuclear g factor, $g \approx Z/A$, the gyromagnetic ratio of a nuclear level in a rotational nuclide is sensitive to the pairing of nucleons in that state. Hence, variations of level g factors in a given rotational band are expected to reflect mainly rotational alignment mechanisms and, as such, are manifestations of the same phenomena displayed in the "backbending plot" which, as a function of rotational frequency, exhibits either the differential moment of inertia or the aligned angular momentum.[1–4] Whereas the yrast sequences of the even isotopes $^{156-164}$Er show strong backbending between spins of 10^+ and 16^+, none is observed up to these spins in the even $^{166-170}$Er nuclides. Of these latter isotopes, ^{166}Er displays a marked "up-bending." The yrast states in all these even-even Er isotopes can be understood in terms of the interaction and/or crossing of the ground-state band (having no unpaired nucleons) and the S band built on two unpaired $i_{13/2}$ neutron quasiparticles with their spins aligned in the direction of the collective rotational angular momentum. The variety of behavior in the yrast sequences of these even Er isotopes can be attributed to variations in the strength of the coupling between the ground and S bands.[5,6] Furthermore, the oscillatory nature of the changes in the interaction strength with neutron number can be reproduced by Hartree-Fock-Bogoliubov (HFB) calculations which show that strength to depend rather sensitively on the Fermi level as it moves through the $i_{13/2}$ subshell.[5–7] Relatively recent measurements[8,9] of the g factors of individual excited states in ^{166}Er observed the gyromagnetic ratios of the levels in its ground-state band (gsb) to decrease rather strongly and monotonically with increasing level spin (up to $J_i^\pi = 10_1^+$). The observed monotonic decrease of the level g factors in ^{166}Er may therefore be linked to a strong interaction between the ground and $\nu(i_{13/2})^2$ S bands. Some support for this interpretation is suggested by the excellent agreement between the experimentally measured yrast level g factors in ^{166}Er (Refs. 8 and 9) and the cranked Hartree-Fock-Bogoliubov (CHFB) calculated predictions of Ansari *et al.*[3]

From another perspective, stimulated by the work of Yoshinaga *et al.*,[10] who showed that "anharmonicities" attributed[11,12] to the band structure of ^{168}Er from comparisons of experiment with the *sd*-boson interacting boson model (IBM) could be largely resolved by inclusion of the g boson, considerable attention has also been given of late to the application of the IBM to the middle rare-earth rotational nuclei, with special interest focused on the role of the hexadecapole (g) bosons[10,13,14] in describing the observed nuclear properties. As a concomitant of g-boson participation, an additional degree of freedom is introduced that offers the possibility of accommodating large variations in the g factors of levels in the gsb through a first-order $M1$ operator. Although, in the SU(3) limit of the *sdg* IBM, any variation in level gyromagnetic ratios that might otherwise be affected through inclusion of the g boson is effectively "locked out" when the number of bosons, N, becomes large in the rotor limit,[13] Kuyucak and Morrison[14] have shown that, away from the SU(3) IBM limiting symmetry, level g-factor variations in the gsb become possible even in the large-N rotor limit, and, by appropriate choice of parameters, the variation in gyromagnetic ratios observed experimentally in ^{166}Er (Refs. 8 and 9) can be reproduced reasonably well in their *sdg*-boson calculations.[14] However, it remains an open and crucial question as to whether the *sdg*-boson IBM in this form can describe g-factor variations in the rare-earth rotors in a consistent fashion.

While the nuclear structure bases underlying the separate CHFB (Refs. 3–7) and IBM *sdg*-boson[14] approaches seem disparate *extrinsically*, it would be of considerable interest to assess and delineate the extent to

which they actually differ *intrinsically,* particularly as the high-spin g boson may be emulating some of the effects of the higher-spin unique parity orbits.[15]

In view of the foregoing interest in the nuclear structure of nuclei near ^{166}Er from rather diverse theoretical approaches, we have extended our transient field precession studies to the measurement of gyromagnetic ratios of individual levels in the ground-state bands of ^{168}Er and ^{164}Dy (a neighboring even-even isotope and isotone of ^{166}Er, respectively), which we report here. Some aspects of this work have already been reported.[16] Our present results for ^{168}Er and ^{164}Dy are compared with the corresponding empirical results for ^{166}Er (Refs. 8 and 9) and assessed in terms of cranked Hartree-Fock-Bogoliubov calculated predictions, the most recent of which[4] were prompted directly by the presentation[16] of our experimental findings.

II. EXPERIMENTAL PROCEDURES

As the experimental procedures and techniques utilized in the present transient field (TF) nuclear precession measurements paralleled those described in earlier publications,[8,17–19] only those particulars specific to the present investigations are outlined here.

The states of interest in both ^{164}Dy and ^{168}Er were populated by multiple Coulomb excitation using ^{58}Ni projectiles from the Australian National University 14UD Pelletron tandem accelerator. As a result of the patterns of level populations and cascade feeding following heavy-ion multiple Coulomb excitation of good-rotor nuclides, as described in detail in Ref. 8, two separate complementary measurements were required to measure the g factors of interest in each of these rare-earth isotopes. In the case of ^{164}Dy, TF precessions were measured using ^{58}Ni projectile energies of 220 and 160 MeV, runs I and II, respectively, while ^{58}Ni beam energies of 220 and 150 MeV were employed in the ^{168}Er studies (runs III and IV, respectively).

In each study, an enriched elemental target was rolled to the desired thickness and carefully pressed onto a previously annealed Fe foil, using a thin evaporated flashing of natural In metal as a convenient, innocuous adhesive. A nonperturbative layer of Pb (sufficient to stop the recoiling target ions) was evaporated on the downstream side of the Fe foil. The entire target assembly was then pressed onto a 15 μm Cu backing (using another In flashing) that provided both added mechanical support and improved thermal conduction away from the beam spot.

Separate targets were made for the lower- and higher-energy experimental runs in each of the ^{164}Dy and ^{168}Er studies. The thicknesses of all four strata in each compound target were obtained by areal-weight measurements after each stage of target fabrication, and, as well, by Rutherford scattering of 3.0-MeV protons from the University of Melbourne 5U Pelletron accelerator. The results of the two sets of measurements on each of the four targets were in good agreement. Target layer thicknesses, target isotopic enrichments, and other particulars are summarized in Table I. All composite targets were cooled during bombardment; target temperatures were maintained below 0°C.

Two pairs of intrinsic Ge γ-ray detectors were placed at $\pm 65°$ and $\pm 115°$ to the beam direction to provide near-optimum sensitivity for the precession measurements of all states of interest, each of which deexcite via $E2$ transitions. In all four experimental runs, the backward pair of detectors ($\pm 115°$) were positioned so that both intercepted the same solid angle at the target; similarly, the two Ge detectors of the forward pair were placed so as to have matched solid angles.

Gamma rays registered in each detector were recorded in coincidence with backscattered projectile ions detected in a common annular Si particle counter (angular range 146°–166°). This coincidence requirement ensured that all recorded events were associated with forward recoiling target nuclei, with their spins aligned to a high degree in the plane, normal to the beam axis. In the 220-MeV runs, the events recorded pertained to ^{164}Dy and ^{168}Er ions moving in a narrow forward cone (half-angle $\sim 8°$) with mean velocities $\sim 0.039c$ on entry to the polarized Fe layer. In the lower-energy bombardments, the corresponding target ions recoiled in a similarly narrow forward cone and entered the Fe substrate of the target with mean initial speeds of $\sim 0.031c$. Data were stored in an event-by-event mode.

The ferromagnetic foil was polarized by an external magnetic field of ~ 0.05 T (sufficient to ensure saturation of the Fe layer) applied in a direction normal to the reaction plane. Effective magnetic shielding, provided by a soft iron cone placed between the target and the annular detector, made beam-bending effects negligible.

TABLE I. Measured strata thicknesses of composite targets used in present study.

Target nuclide	Target thickness (mg/cm^2)	Projectile beam energy (MeV)	Thickness (mg/cm^2) In	Fe	Pb
^{164}Dy	2.6±0.1[a]	220	0.21±0.04	4.2±0.1	17.5±0.5
^{164}Dy	2.8±0.1[a]	160	0.14±0.03	2.4±0.1	28±1
^{168}Er	2.3±0.1[b]	220	0.14±0.03	4.1±0.1	13±1
^{168}Er	2.3±0.1[b]	150	0.24±0.04	2.4±0.1	17±1

[a]Elemental composition (as quoted by supplier): 95.68% ^{164}Dy; 3.08% ^{163}Dy; 0.84% ^{162}Dy; 0.37% ^{161}Dy; 0.04% ^{160}Dy; <0.02% ^{158,156}Dy.

[b] Elemental composition (as quoted by supplier): 0.61% ^{170}Er; 95.47% ^{168}Er; 2.44% ^{167}Er; 1.44% ^{166}Er; 0.04% ^{164}Er; <0.02% ^{162}Er.

Unperturbed particle-γ-ray angular correlations of all deexcitation transitions were measured using the same detectors, beams, targets, target-to-detector distances, and coincidence restriction employed in the TF precession measurements, save that one γ-ray detector was positioned, in turn, at five different forward angles, while the other three HP Ge detectors were held fixed and served as monitors. After each run, the relative γ-ray detection efficiencies of the Ge detectors were determined by placing ^{133}Ba, ^{152}Eu, and ^{182}Ta sources at the target position.

In the present experiments, as was the case in our earlier g-factor studies of ^{166}Er (Ref. 8), $\sim$7 d of beam time were required to obtain the present results for each of the nuclides ^{164}Dy and ^{168}Er. Of this, $\sim$4 d were allocated to the higher-energy precession measurements (runs I and III), $\sim$2 d to the lower-energy runs (runs II and IV), and $\sim$1 d to measuring the angular correlations at the respective beam energies. This approximate apportionment of beam time proved optimum for measuring the relative g factors of levels in the ground-state bands as precisely as possible in runs of $\sim$1 week duration.

III. ANALYSIS

The procedures followed in the analyses of the present TF precession data were those developed earlier[8,17–19] for the extraction of the relative g factors of individual excited states in a given nuclide from *simultaneously* measured transient field asymmetries. The analysis takes proper account of both (i) the TF precessions in the directly populated higher-excitation states which cascade-feed down to the lower-excitation levels, and (ii) the consequences of decays in flight of the shorter-lived states until the nucleus emerges from the ferromagnetic foil. These two effects are not separable.

Although states in the ground bands as high as the 14_1^+ in both nuclides under investigation were populated in the 220-MeV bombardments, direct populations of levels higher than the 10_1^+ were not strong enough to allow their gyromagnetic ratios to be obtained with useful precision or accuracy. Similarly, whereas states up to the 8_2^+ were observed in the γ bands, only the 2_2^+ level g factors could be extracted.

While states up to and including the $J_i^\pi = 10_1^+$ in the ground-state bands and the $K=2$ bandheads (2_2^+) in the two nuclides under study received sufficient direct population to extract meaningful TF precessions for them in the 220-MeV ^{58}Ni bombardments (runs I and III, respectively) of ^{164}Dy and ^{168}Er (although higher excited states were seen to be populated reasonably strongly), excessive feeding to the 4_1^+ states in both nuclides precluded extraction of their g factors in these higher-energy bombardment runs. However, in the two lower-energy bombardments of these nuclides (runs II and IV), indirect population (feeding) of the 4_1^+ state in both cases was significantly reduced, while the 6_1^+ states were still populated sufficiently strongly to allow precise TF precession data to be obtained for *both* states.

Meaningful measures of the gyromagnetic ratios of the 2_1^+ states in both ^{164}Dy and ^{168}Er could not be deduced from the present data for the 2_1^+-to-0_1^+ transitions, despite the more moderate proportion of indirect populations of these levels in the lower-energy bombardment studies (runs II and IV, respectively). As was similarly the case in our earlier study of the gyromagnetic ratios of the corresponding excited states in ^{166}Er (Ref. 8) this could be traced to several effects related directly to the relatively low energy, ≤ 81 keV, of these 2_1^+-to-0_1^+ transitions: (i) their high internal-conversion coefficients ($\alpha_T \approx 6.6$) lead to rather low relative effective γ-ray yields for these first excited 2^+ states, and, thus, to rather poor experimental sensitivity to TF precessions of the nucleus in these states, (ii) the relatively high absorption of these low-energy γ rays in the target layers distorts the angular correlations over the range of oblique acceptance angles intercepted by the γ-ray detectors in the precession measurements, and (iii) the 2_1^+ levels are long lived ($\tau > 2$ ns) and are most likely to be deoriented by residual electric field gradients in the Pb backings. The combination of these effects rendered virtually nil the sensitivity of the precession data obtained to the g factors of these 2_1^+ states.

Unperturbed particle-γ-ray angular correlations were calculated for all transitions of interest for our experimental geometry employing alignment tensors obtained using the Winther-de Boer multiple Coulomb excitation code.[20] As the alignment tensor values calculated for states in even-even nuclei are rather insensitive to the matrix elements selected, the required matrix elements were taken from previously measured (or lifetime-inferred) $B(E2)$ values,[21–23] where known, and the remainder from rotor model specifications. However, as calculation of the angular correlation of each transition also involves the relative direct populations of the levels, and, as the relative direct level populations calculated by means of the Winther-de Boer code[20] *are* matrix element sensitive, these relative populations were taken from intensities determined from the present measured unperturbed angular correlations (corrected for internal conversion and relative γ-ray detection efficiencies).

IV. EXPERIMENTAL RESULTS

Partial level schemes incorporating all states populated and all transitions observed in the present studies are shown for ^{164}Dy and ^{168}Er in Figs. 1 and 2, respectively; the fraction of the overall population of each level that was *direct*, at both the higher and lower bombarding energies in both nuclides, is designated in these figures.

Representative spectra of deexcitation γ rays recorded in coincidence with backscattered ^{58}Ni projectiles in each of the four experiments are presented in Figs. 3 and 4. Particularly noticeable in these spectra are the significantly reduced populations of the higher-excited states in the lower-energy bombardments, which allowed the extraction of g factors associated with the lower-lying excited levels with relatively small corrections for feeding effects.

Comparisons of the predicted angular correlations with those measured are shown in Figs. 5 and 6 for ^{164}Dy and

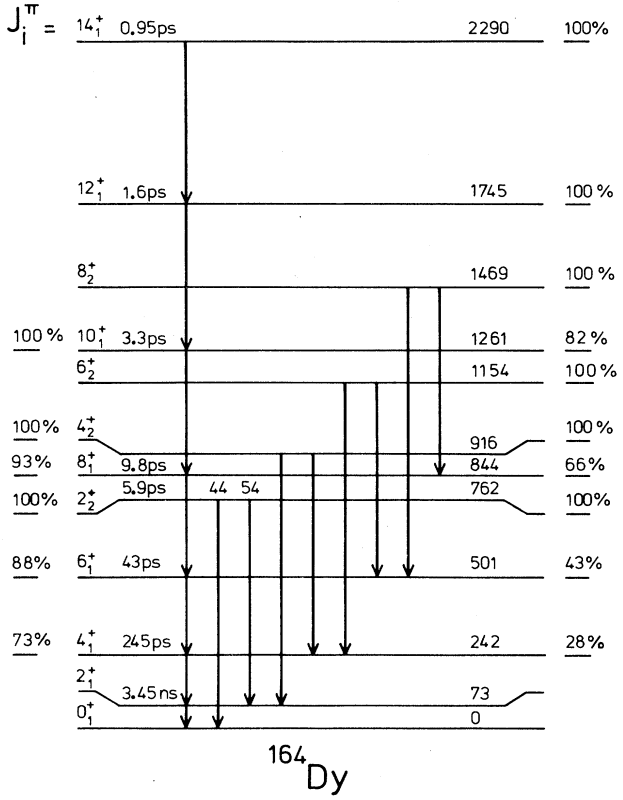

FIG. 1. Partial level and decay scheme of ^{164}Dy incorporating all states and transitions of interest. All transitions shown were observed in the present work. Transition branching ratios are given in percent. States are labeled by percent direct Coulomb excitation level population in 220- and 160-MeV ^{58}Ni bombardments (right-hand and left-hand sides of levels, respectively), see text for details. Known level mean lives are specified; excitation energies of levels are given in keV.

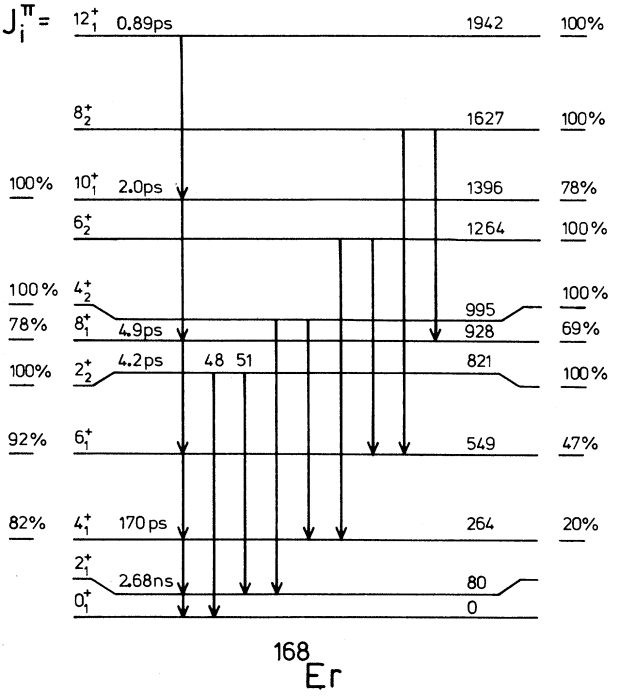

FIG. 2. Same as for Fig. 1, but for ^{168}Er at ^{58}Ni ion bombardments of 220 and 150 MeV.

^{168}Er, respectively. The agreement is quite good in all cases. The only free parameters in the "fits" of these calculated angular correlations to the experimental ones are the overall strength of the transitions and the offset angle of the 0° detector reference axis relative to the actual incident beam direction. In all cases, the offset angle which best fit all simultaneously recorded angular correlation data was less than 2°.

Tables II and III provide summaries of the particulars of the present set of transient field precession measurements for ^{168}Er and ^{164}Dy, while Table IV presents the analyzed results, the present extracted *relative* g factors of levels, and the adopted *absolute* g factors (obtained by normalization to the few earlier reported measured gyromagnetic ratios, where available) for both nuclides. As the previously measured gyromagnetic ratios of levels, to which the present results could be normalized to obtain these *absolute* g factors, have fractional errors assigned that are considerably larger than those associated with our measured precession results for corresponding levels, it is upon the present *relative* gyromagnetic ratios, *simultaneously* measured for all levels in each separate nuclide, that most reliance rests.

TABLE II. Experimental details.

Target nucleus	^{58}Ni beam energy (MeV)	T_{tgt}[a] (ps)	T_{Fe}[b] (ps)	E_i[c] (MeV)	E_e[c] (MeV)	$\langle v/v_0 \rangle$[c]	Run label
^{164}Dy	220	0.12	0.89	116	9	2.8	run I
^{164}Dy	160	0.16	0.46	76	19	3.0	run II
^{168}Er	220	0.10	0.80	123	12	3.0	run III
^{168}Er	150	0.13	0.48	73	18	3.2	run IV

[a]Mean time of recoil nucleus in target layer.
[b]Mean transit time of recoil nucleus through ferromagnetic foil.
[c]Mean incident energy (E_i) and emergent energy (E_e) of recoil nucleus into and out of ferromagnetic foil, respectively; $\langle v/v_0 \rangle$ is the mean velocity of the recoiling ions whilst in the ferromagnetic host; $v_0 = c/137$, is the Bohr velocity.

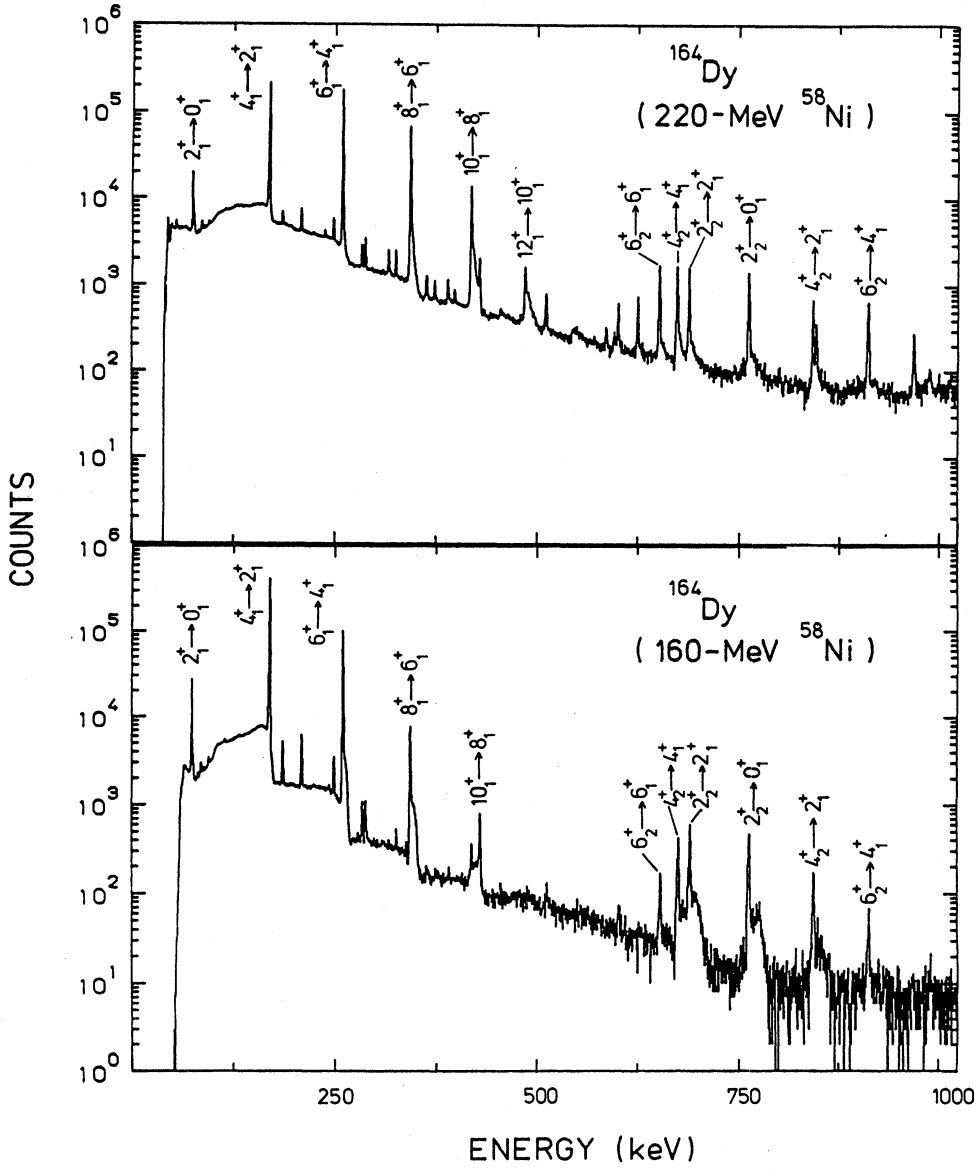

FIG. 3. Representative spectra of deexcitation γ rays detected at 65° to the beam direction in coincidence with backscattered projectiles following Coulomb excitation of levels in ^{164}Dy by 220-MeV ^{58}Ni ions (upper portion) and 160-MeV ^{58}Ni ions (lower portion). Transitions are labeled by $J_i^\pi \rightarrow J_f^\pi$. Chance coincidences have been subtracted.

Although we have chosen not to rely upon any particular parametrization of the TF to obtain *absolute* g factors in ^{164}Dy and ^{168}Er, a large body of data for rare-earth nuclides traversing polarized Fe hosts was included in the TF parametrization work of the Chalk River group[26] and, within its assigned uncertainties, their parametrization would be expected to provide a reliable calibration for Er and Dy ions traversing fully magnetized Fe over the ion velocity ranges which pertained in our measurements. The $g(6^+)$ values for ^{164}Dy and ^{168}Er, obtained by calibration using the Chalk River parametrization, are 0.21 ± 0.02 and 0.345 ± 0.022, respectively. These values agree within experimental errors with those adopted for the 6^+ states (Table IV). In the case of ^{164}Dy, however, the 6_1^+ g factor obtained using the Chalk River parametrization[26] is significantly smaller than the values of $g(2_1^+)$ measured previously.[24] It can be seen from Table III that the observed precessions for all states in ^{164}Dy in both measurements are smaller than the corresponding values in ^{168}Er and ^{166}Er (see also Ref. 8). It is very improbable that this could be due to either (i) some kind of discontinuity in the TF strength as a function of atomic

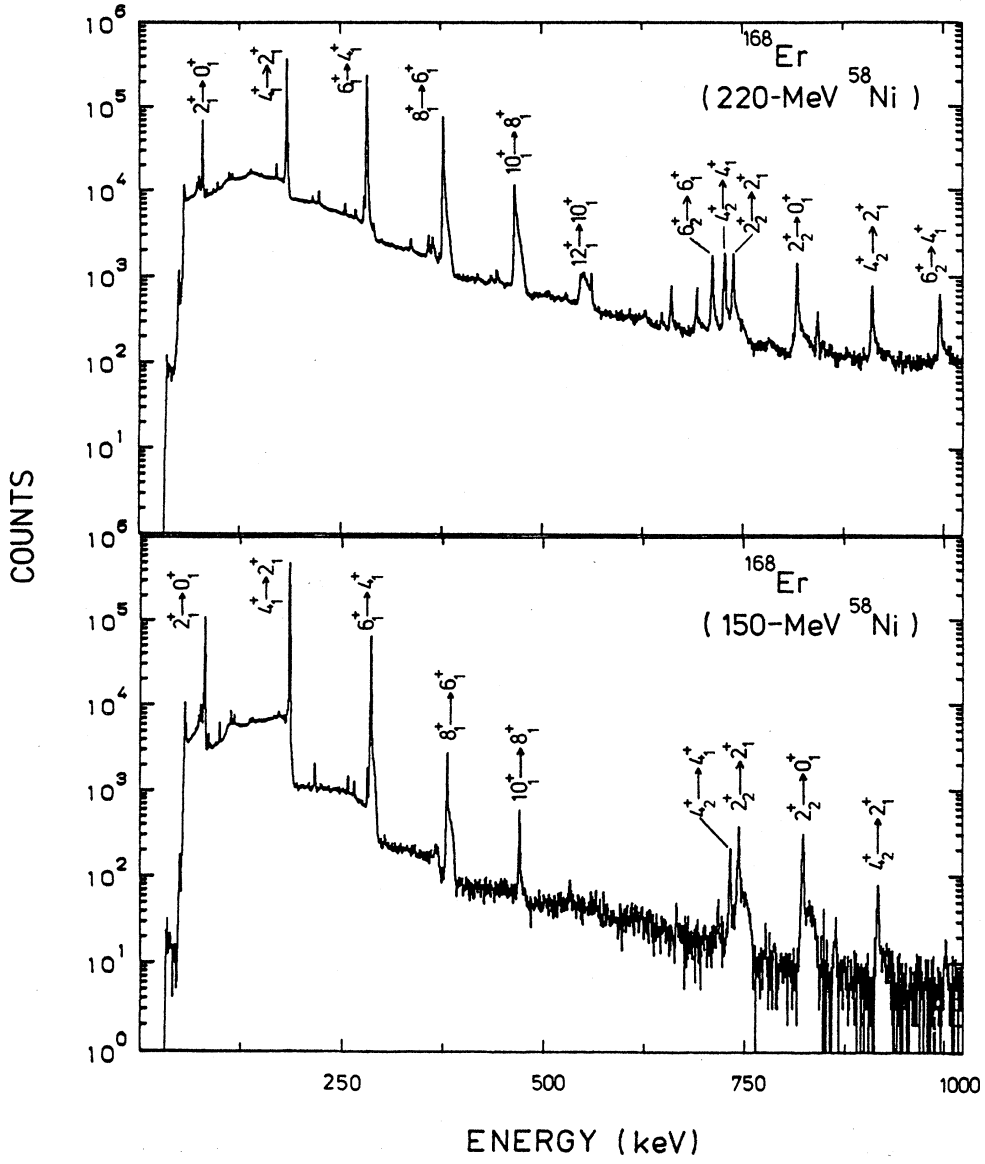

FIG. 4. Representative deexcitation γ-ray spectra recorded for ^{168}Er in the present work for 220- and 150-MeV ^{58}Ni bombardments (upper and lower portions, respectively); all other particulars as per caption of Fig. 3.

number between Dy and Er (Ref. 26) [similar, for example, to that found in the region around Os and Pt (Ref. 27)], or (ii) an experimental problem, such as loss of foil magnetization in *both* of the ^{164}Dy experiments, but in *none* of the four ^{166,168}Er measurements which were performed under almost identical experimental conditions. Rather, our overall data set suggests that $g(6_1^+)$ in ^{164}Dy may be considerably smaller than the previously measured values reported for the 2_1^+ state. Unfortunately, the only available independently measured[25] g factor to which we can normalize our results has a large experimental uncertainty and a value which lies between the previous 2_1^+ results and the $g(6_1^+)$ value inferred from our data using the Chalk River parametrization. A more precise *absolute* calibration of our g-factor values for ^{164}Dy requires an independent, precise determination of $g(4_1^+)$ or $g(6_1^+)$. As such a measurement is outside the scope of the present work, the discussion of ^{164}Dy which follows focuses upon the measured *relative* gyromagnetic ratios in the ground-band state (gbs) of this nuclide.

Finally, shown diagrammatically in Fig. 7 are the present and previous gyromagnetic ratio results for levels in the ground bands of ^{164}Dy and ^{168}Er. For completeness and to reveal the striking constrast, this figure also

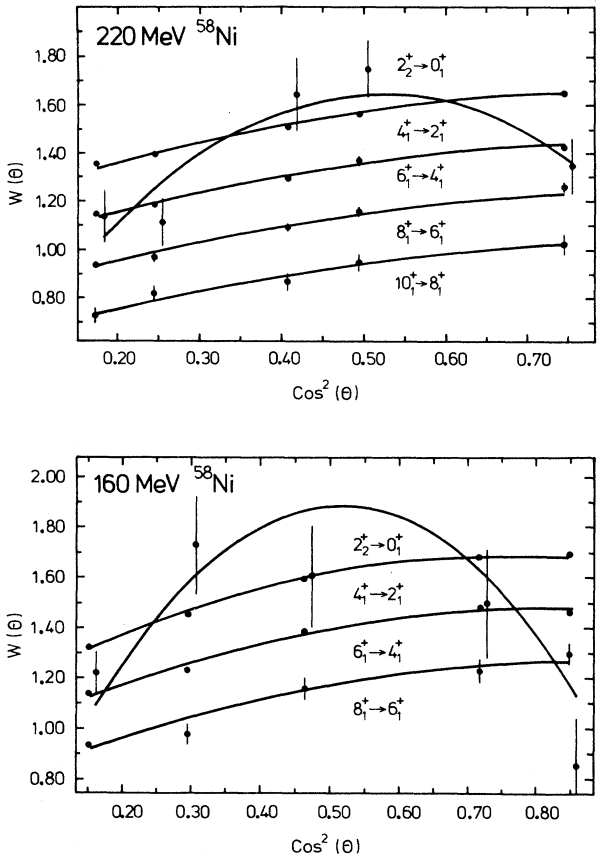

FIG. 5. Measured (data points) deexcitation γ-ray angular correlations (see text) of designated transitions in ^{164}Dy in 220- and 160-MeV ^{58}Ni ion bombardments (upper and lower portions, respectively). The solid curves are not fits to these data, they represent the correlations calculated by means specified in Secs. III and IV of the text. Transitions are labeled by $J_i^\pi \rightarrow J_f^\pi$. For clarity of presentation, the results for the various transitions have been offset from one another.

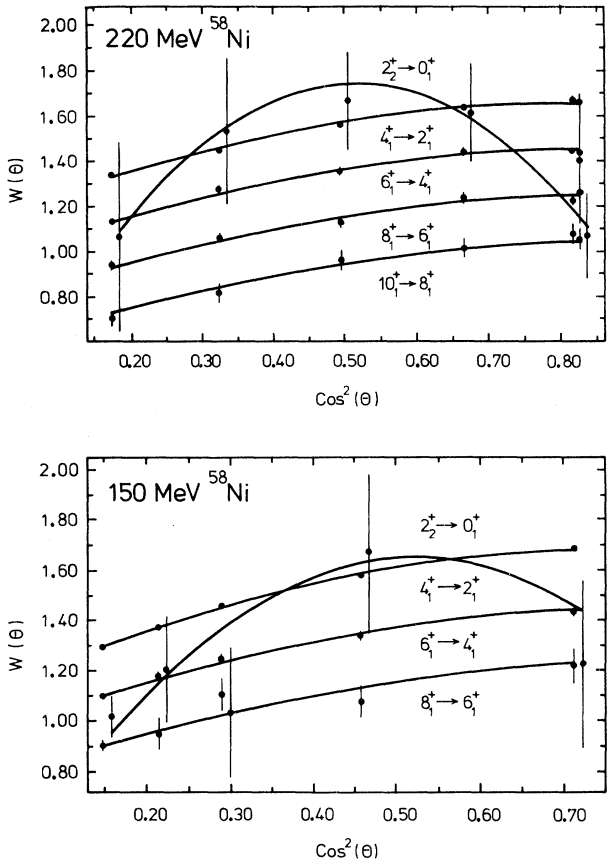

FIG. 6. Same as for Fig. 5, but for ^{168}Er at ^{58}Ni ion bombardments of 220 and 150 MeV (upper and lower portions, respectively).

presents the earlier reported[8,9] measured g factors of corresponding states in ^{166}Er (the results of the two ^{166}Er studies[8,9] have been combined and averaged). In the cases of ^{164}Dy and ^{168}Er, each of the present measured g factors for the 4_1^+ to 10_1^+ levels are displayed with two error estimates; the larger error bars include uncertainties in the *absolute* calibration of the measured gyromagnetic ratios, whereas the uncertainties in the present *relative* measurements, also shown, are considerably smaller. In Fig. 7, comparisons are made between the experimental results and the predictions of various models to be discussed in Sec. VI. It should be stressed that what is presented in this figure, for both the experimental measurements and the calculations with which they are compared, are the gyromagnetic ratios of levels *relative* to that of the 2_1^+ state in the *same* nuclide—that is, $g(J)/g(2_1^+)$ vs J, but *not* $g(J)$ vs level spin J.

V. COMPARISON OF RESULTS

The rather dramatic contrast between the systematic behavior exhibited by the measured gyromagnetic ratios of corresponding levels in the ground-state band of ^{166}Er and that of ^{168}Er is evident in Fig. 7. While the present measured gyromagnetic ratios of all of the low-spin yrast states up to and including $J^\pi = 10^+$ in ^{168}Er appear fully consistent with being the same, the g factors of the corresponding levels in ^{166}Er display the marked departure from constancy noted earlier.[8]

To compare and classify the g-factor trends in the three nuclides under discussion more objectively, it is helpful to fit the gsb g factors using a parametrization suggested by Chen and Frauendorf[2]

$$g(J) = g_0(1 + \alpha J^2) \ . \tag{1}$$

Ground-band level g factors from 2_1^+ to 10_1^+ were included in the fits for ^{166,168}Er. For ^{164}Dy, while the present measured relative g factors for the 4_1^+ to 10_1^+ states were

TABLE III. Measured transient field precessions of designated states in ^{164}Dy and ^{168}Er.

Run	Nucleus	State (J_i^π)	ϵ_{14}[a] ($\times 10^{-3}$)	ϵ_{23}[b] ($\times 10^{-3}$)	S_{14}[c]	S_{23}[c]	$\langle\Delta\Theta_{14}\rangle$[d] (mrad)	$\langle\Delta\Theta_{23}\rangle$[d] (mrad)
I	^{164}Dy	6_1^+	−18.4(8)	+17.6(12)	−0.73(3)	+0.79(3)	26.9(38)	18.8(46)
		8_1^+	−16.4(13)	+19.1(18)	−0.69(3)	+0.75(3)	21.2(39)	25.7(49)
		10_1^+	−19.4(29)	+18.8(37)	−0.66(4)	+0.71(5)	32.8(89)	26.4(85)
		2_2^+	−63(9)	+87(12)	−2.65(12)	+2.90(12)	25.7(35)	32.6(47)
II	^{164}Dy	4_1^+	−13.9(7)	+14.3(9)	−0.97(2)	+1.03(2)	15.0(11)	14.9(16)
		6_1^+	−9.7(14)	+19.0(17)	−0.81(2)	+0.85(2)	12.4(21)	9.7(25)
		8_1^+	−6.4(48)	+13.8(58)	−0.74(3)	+0.77(3)	5.3(77)	22.8(93)
		2_2^+	−16(17)	+31(22)	−2.79(13)	+2.91(13)	6.1(66)	11.3(80)
III	^{168}Er	6_1^+	−25.1(7)	+26.7(8)	−0.77(4)	+0.80(4)	34.3(47)	33.1(50)
		8_1^+	−21.8(11)	+23.8(14)	−0.73(4)	+0.75(4)	32.2(38)	36.5(43)
		10_1^+	−19.1(25)	+24.5(32)	−0.69(4)	+0.72(4)	31.1(91)	34.6(78)
		2_2^+	−106(12)	+98(14)	−2.91(12)	+3.05(12)	40.7(45)	35.9(51)
IV	^{168}Er	4_1^+	−20.6(5)	+20.5(7)	−0.99(2)	+1.05(2)	20.5(7)	19.3(9)
		6_1^+	−17.8(13)	+17.9(17)	−0.81(2)	+0.86(2)	21.6(19)	21.5(22)
		2_2^+	−51(22)	+43(25)	−2.63(13)	+2.77(13)	21.2(90)	16.9(97)

[a]Transient field asymmetry measured using the forward detector pair, $\epsilon=(1-\rho)/(1+\rho)$, where $\rho=\{N\uparrow(+)N\downarrow(-)/N\downarrow(+)N\uparrow(-)\}^{-1/2}$, with $N\uparrow(\downarrow)$ the normalized counts observed in the field up (down) direction in the detector pair at $+(-)65°$.
[b]Same as for footnote a of this table, except for backward pair of detectors at $+(-)115°$.
[c]Logarithmic derivative of unperturbed γ-ray angular correlation of observed $E2$ transition from each level, evaluated at detection angle, for forward detector pair S_{14} and backward detector pair S_{23}. Errors reflect uncertainties in the measured intensities of transitions.
[d]Precessions calculated from ϵ_{ij} and S_{ij} corrected for feeding and decay-in-transit effects (see text).

included, that of $g(2_1^+)$ was excluded because it could not be combined precisely with the present data. The results of these fits were

$$\alpha(^{164}\text{Dy})=(-21\pm15)\times10^{-4}\ ,$$
$$\alpha(^{166}\text{Er})=(-40\pm2)\times10^{-4}\ ,$$
$$\alpha(^{168}\text{Er})=(1.6\pm2.8)\times10^{-4}\ .$$

Comparing the cases of ^{164}Dy and ^{166,168}Er, although the present Dy g-factor results are not the statistical equal of those obtained for these two Er isotopes (mainly because the Dy TF precessions are smaller), it is nevertheless evident from the fitted α values that some diminution of the ^{164}Dy gbs level g factors with increasing spin may be suggested, but that the effect is not as dramatic as observed for the corresponding states of ^{166}Er.

VI. DISCUSSION OF RESULTS

A. g factors in ^{166,168}Er as a probe of rotational alignment

Following the prescription of Frauendorf,[1] and Chen and Frauendorf[2] if the backbending is interpreted as the crossing between the ground-state band and an aligned two-quasiparticle band, the change of the level g factor with increasing spin can be related to the aligned angular momentum extracted from the experimental energy spectrum. Usually, the ground band below the backbend is parametrized in terms of the Harris polynomial[6]

$$I_{xg}(\omega)=\omega I_0+\omega^3 I_1\ , \tag{2}$$

where $I_{xg}=[\bar{I}(\bar{I}+1)]^{1/2}$, $\bar{I}=(J_i+J_f)/2$, and, in an even nucleus, ω is one-half the energy of the $J_i\rightarrow J_f$ transition. Figure 8 shows the trends in values of I_0 and I_1 for the even Dy and Er isotopes, estimated by fitting the experimental level spectra of the ground-state bands up to their 10_1^+ states. While the values of I_0 show a smooth variation with neutron number in both Dy and Er, I_1 displays a maximum at $N=98$, which, as discussed by Bengtsson and Frauendorf,[5] corresponds to a maximum in the interaction between the g and S bands. To estimate g factors, Chen and Frauendorf[2] ascribe the angular momentum $\omega\delta I_0+\omega^3\delta I_1$ corresponding to the deviations δI_0, δI_1 of I_0, and I_1 from the "smooth background" $\bar{I}_0$ and $\bar{I}_1$ (in Fig. 8) to the $i_{13/2}$ quasiparticles causing the bump at $N=98$, and obtain

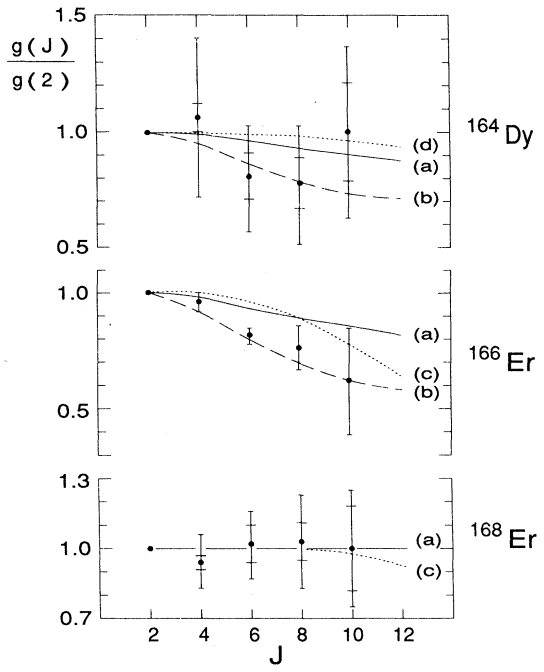

FIG. 7. Experimental g-factor ratios $g(J)/g(2_1^+)$ in the ground-state bands of ^{164}Dy and ^{166,168}Er compared with various theoretical calculations. Results for ^{164}Dy and ^{168}Er are derived from Table IV, those for ^{166}Er are combined averaged values from Refs. 8 and 9. Full error bars on the data points include uncertainties in the *absolute* g factors; the smaller error estimates also shown for the $J=4_1^+$ to 10_1^+ levels in ^{164}Dy and ^{168}Er indicate uncertainties in the present *relative* g-factor measurements. Calculations are discussed in Sec. VI. (a) Present semiempirical calculations using the method of Chen and Frauendorf[2], (b)–(d) CHFB calculations from Refs. 3,4, and 28, respectively.

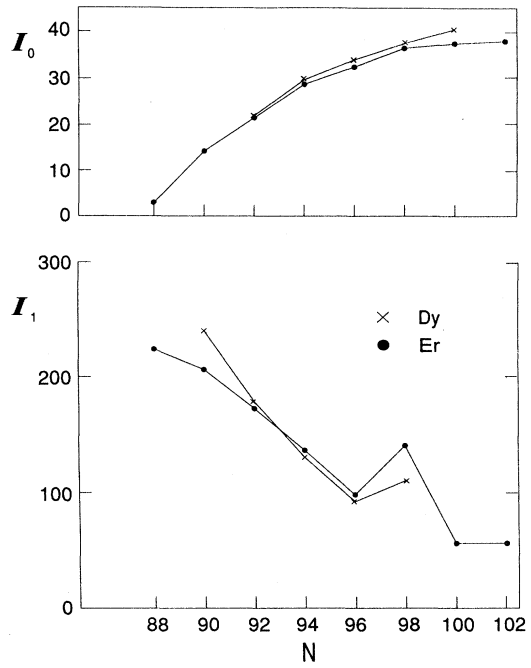

FIG. 8. Systematics of experimental values of the Harris polynomial parameters I_0 and I_1 for isotopes of Dy and Er, obtained as described in Sec. VI A.

$$g(\omega)=\bar{g}+(g_j-\bar{g})[(\delta I_0+\omega^2\delta I_1)/(I_0+\omega^2 I_1)]\ , \quad (3)$$

where $\bar{g}$ is the average collective g factor and g_j is the g factor of the aligned quasiparticles.

To determine $g(\omega)$ requires reasonable estimates of $\bar{g}$, g_j, δI_0, and δI_1. For the mean collective g factor, $\bar{g}$, we take the g value of the 2_1^+ state of the nucleus, and for g_j we assume that of the $i_{13/2}$ neutrons quenched by the usual factor of 0.7, so that $g(i_{13/2})=-0.17$. Values of δI_0 and δI_1 may be inferred from Fig. 8. Gyromagnetic ratios given by Eq. (3) are compared with experiment in Fig. 7. Although there is an element of subjectivity in choosing the "background" values of $\bar{I}_0$ and $\bar{I}_1$, the qualitative variation in g factor behavior in ^{164}Dy, ^{166}Er, and ^{168}Er from Eq. (3) is clear—namely, the g factors in ^{168}Er should be near constant, those in ^{166}Er should show the most pronounced decrease with increasing spin, and in the $N=98$ isotone ^{164}Dy, there should also be a decrease with increasing spin, but less so than in ^{166}Er. This compares favorably with the trends implied by the α values [Eq. (1)] extracted from the data in Sec. V.

While this simple model has difficulty making the decrease of the g factors with increasing spin as marked as observed in ^{166}Er, the qualitative trends of the data for the three nuclides considered are reproduced reasonably well.

B. Cranked Hartree-Fock-Bogoliubov (CHFB) calculations

Several studies of the behavior of level g factors as a function of spin in rotational nuclei have been performed in the framework of CHFB calculations.[3,4,28] Comparisons between the calculations of Refs. 3, 4, and 28 for ^{166,168}Er and ^{164}Dy and our experimental results are shown in Fig. 7. Note that none of these calculations[3,4,28] has been simultaneously or consistently applied to all three nuclides. While these three calculational studies differ in detail, such as the residual interactions chosen, and their predictions of the spin variations of the g factors also differ significantly, they are unanimous in attributing the spin variations of the level magnetic moments to rotational alignment effects. As noted in our earlier publication[8] there is a remarkably close concurrence between the measured gyromagnetic ratios in ^{166}Er and the calculated predictions for this nuclide of Ansari *et al.*[3] Nevertheless, the well-known shortcomings of the CHFB method[3,29,30] (that the number of nucleons and the total angular momentum are conserved only *on average*) may conduce to treatment of this agreement between experiment and CHFB calculations with some measure of circumspection. Indeed, Ansari *et al.*[3] did examine the effect of neglecting the projection of good nucleon number by comparing calculations of the pairing gaps as a function of spin in ^{158}Dy in the cases of variation without

TABLE IV. Summary of experimental results.

Nucleus	State (J_i^π)	$\langle\Delta\Theta\rangle$[a] (mrad)	$\frac{\langle\Delta\Theta\rangle}{\langle\Delta\Theta\rangle_{6_1^+}}$	$\langle\Delta\Theta\rangle$[a] (mrad)	$\frac{\langle\Delta\Theta\rangle}{\langle\Delta\Theta\rangle_{6_1^+}}$	$\frac{g^{b}}{g_{6_1^+}}$	g_{previous}	g_{adopted}
		Run I		Run II				
^{164}Dy	2_1^+						0.348(9)[c]	0.348(9)
	4_1^+			14.8(9)	1.31(20)	1.31(20)		0.37(12)
	6_1^+	23.6(29)	1	11.3(16)	1	1	0.28(8)[d]	0.28(8)
	8_1^+	22.9(31)	0.97(18)	12.4(59)	1.10(54)	0.98(17)		0.27(9)
	10_1^+	29.5(61)	1.25(30)			1.25(30)		0.35(13)
	2_2^+	28.2(28)	1.19(19)	8.2(51)	0.73(46)	1.12(18)		0.31(10)
		Run III		Run IV				
^{168}Er	2_1^+						0.321(6)[c]	0.321(6)
	4_1^+			19.9(6)	0.92(7)	0.92(7)	0.303(37)[c]	0.303(37)
	6_1^+	33.7(34)	1	21.6(14)	1	1		0.328(46)
	8_1^+	34.1(28)	1.01(13)			1.01(13)		0.331(63)
	10_1^+	33.1(59)	0.98(20)			0.98(20)		0.322(80)
	2_2^+	38.6(34)	1.15(15)	19.2(66)	0.89(31)	1.10(14)		0.361(69)

[a]Weighted average of nuclear precessions measured in forward and backward detector pairs, from Table III. The 4_1^+ state precessions for both ^{164}Dy and ^{168}Er have been corrected for the small additional rotations undergone in the external polarizing field (0.2 and 0.1 mrad, respectively).
[b]Using $g \propto \langle\Delta\Theta\rangle$.
[c]Weighted average of values reported in Ref. 24.
[d]Reference 25.

number projection and of variation after number projection. It was on the basis of these calculations and comparisons that they concluded that projecting good particle number could be neglected without changing their calculated results greatly. However, as they did not perform test calculations to assess the importance of projecting good *angular momentum* before and after variation, it might be argued that this omission in the cranked Hartree-Fock-Bogoliubov approach could limit severely the reliability of such CHFB calculations of g factors. In rotational nuclei which have a band crossing with a $\nu(i_{13/2})^2$ rotationally aligned band, the effect of angular momentum averaging on calculated g factors would be to overestimate their reduction at low spins well below the band crossing. In this regard, the CHFB calculations of Ansari *et al.*[3] predicted an even more marked decrease of the g factors of the lower-spin gsb states as a function of increasing level spin (up to and including $J_i^\pi = 10_1^+$) in the even-even Sm isotopes which experiments[19,26] have failed to confirm in the cases of ^{152,154}Sm. In comparison with experiment, Ansari *et al.*[3] noted that their calculated g factors were always smaller than experiment and that their calculated energy spectra did not reproduce the backbending; they took these shortcomings as evidence of the need to include a quadrupole pairing term in the residual interaction.

After the results of our experimental studies were presented in summary form,[16] Sugawara-Tanabe and Tanabe[4] were prompted to calculate the yrast level g factors as a function of spin across the even-even $^{158-170}$Er isotopes using a CHFB approach in which the strength of the quadrupole pairing term in their Hamiltonian was adjusted to reproduce the backbending. While their calculations, like those of Ansari *et al.*[3], did not project good angular momentum before variation, their calculated level g factors nevertheless agree very well with the experimental values, where available. However, since the variation of g factors and the energy spectra (backbending) are both intimately related to rotational alignment mechanisms and the residual interactions had been adjusted to "reproduce the backbending" in their calculations[4] it would seem somewhat premature to conclude that the projection of good angular momentum is not at all important. It would be particularly instructive, as we noted earlier[8], to also compare other calculated and experimental properties of levels in these nuclides, such as $E2$ transition rates. As the quadrupole properties of the nucleus depend on its shape and are likely to be sensitive to angular momentum admixtures in the CHFB wave functions,[28] the extra computational effort required to project good angular momentum becomes imperative if reliable $E2$ properties are to be calculated. To our knowledge,

calculations of these relevant $B(E2)$'s have not yet been performed in the CHFB framework.

C. Interacting boson model

The *sdg*-boson interacting boson model approach[14] has already displayed some promise in tracing both the trend and extent of the experimentally established variation of the g factors of the $J^{\pi} \leq 10^{+}$ yrast levels in ^{166}Er.[8,9] It would be particularly interesting and illuminating if such *sdg*-boson IBM calculations were also applied specifically to the present cases of ^{164}Dy and ^{168}Er; certainly, it should prove a significant test of this IBM approach to reproduce the abrupt isotopic and isotonic change in nuclear structure characteristics reflected in the present and earlier[8,9] yrast level g-factor measurements of these three nuclides.

These calculations may be particularly revealing because the *sdg* IBM approach ascribes the g-factor variations to "stretching" (i.e., amplitudes of the boson operators in the intrinsic state change with spin), whereas the CHFB models attribute the g-factor variations to the alignment of a pair of high-spin quasiparticles near the Fermi surface. It is known[31] that the IBM must be extended to include two-quasiparticle excitations in order to describe the high-spin states in deformed and transitional nuclei, i.e., backbending. If the inclusion of two-quasiparticle excitations in the IBM proves essential also for a proper description of the g-factor variations in these neighboring Dy and Er isotopes, it would at least establish some intuitive link between the physical bases of the CHFB and IBM descriptions.

ACKNOWLEDGMENTS

The invaluable hospitality and cooperation extended to us by the staff of the Australian National University 14UD Pelletron Laboratory is appreciated greatly. The technical and related support provided by B. Szymanski, illuminating discussions with Dr. I. Morrison on theoretical aspects, and the aid of A. H. F. Muggleton in target material fabrication proved most helpful. One of us (A.P.B.) acknowledges the support of a National Research Fellowship; while two of us (C.E.D. and G.J.L.) the support of University of Melbourne and Commonwealth Post-Graduate Awards, respectively. This research was supported, in part, by grants from the Australian Research Grants Scheme and Budget Rent-a-Car (Australia).

---

*Present address: Research and Development Division, Mt. Isa Mines Ltd., Mt. Isa, Queensland, Australia 4825.

†Present address: Department of Nuclear Physics, Research School of Physical Sciences, Australian National University, P.O. Box 4, Canberra, Australia 2601.

[1]S. Frauendorf, Phys. Lett. **100B**, 219 (1981).

[2]Y. S. Chen and S. Frauendorf, Nucl. Phys. **A393**, 135 (1983).

[3]A. Ansari, E. Wust, and K. Muhlhans, Nucl. Phys. **A415**, 215 (1984).

[4]K. Sugawara-Tanabe and K. Tanabe, Phys. Lett. B **207**, 243 (1988).

[5]R. Bengtsson and S. Frauendorf, Nucl. Phys. **A314**, 27 (1979).

[6]R. Bengtsson and S. Frauendorf, Nucl. Phys. **A327**, 139 (1979).

[7]R. Bengtsson and J.-Y. Zhang, Phys. Lett. **135B**, 358 (1984).

[8]C. E. Doran, H. H. Bolotin, A. E. Stuchbery, and A. P. Byrne, Z. Phys. A **325**, 285 (1986).

[9]A. Alzner, E. Bodenstedt, J. Gemunden, J. van den Hoff, and H. Rief, Z. Phys. A **322**, 467 (1985).

[10]N. Yoshinaga, Y. Akiyama, and A. Arima, Phys. Rev. Lett. **56**, 1116 (1986).

[11]A. Bohr and B. R. Mottelson, Phys. Scr. **25**, 28 (1982).

[12]T. S. Dumitrescu and I. Hamamoto, Nucl. Phys. **A383**, 205 (1982).

[13]I. Morrison, Phys. Lett. B **175**, **1** (1986), and references therein.

[14]S. Kuyucak and I. Morrison, Phys. Rev. Lett. **58**, 315 (1987).

[15]A. Gelberg, P. von Brentano, and I. Morrison, J. Phys. G **15**, 801 (1989).

[16]C. E. Doran, H. H. Bolotin, A. E. Stuchbery, A. P. Byrne, and G. J. Lampard, in *Proceedings of the International Conference on Nuclear Structure Through Static and Dynamic Moments,* edited by H. H. Bolotin (Melbourne Conference Proceedings Press, Melbourne, 1987), p. 169.

[17]A. E. Stuchbery, C. G. Ryan, H. H. Bolotin, I. Morrison, and S. H. Sie, Nucl. Phys. **A365**, 317 (1981).

[18]A. E. Stuchbery, I. Morrison, L. D. Wood, R. A. Bark, H. Yamada, and H. H. Bolotin, Nucl. Phys. **A435**, 635 (1985); H. H. Bolotin, in Proceedings of the 1984 INS-RIKEN International Symposium on Heavy-Ion Physics, Mt. Fuji, 1985 [J. Phys. Soc. Jpn. Suppl. II **54**, 536 (1985)].

[19]A. P. Byrne, A. E. Stuchbery, H. H. Bolotin, C. E. Doran, and G. J. Lampard, Nucl. Phys. **A466**, 419 (1987).

[20]A. Winther and J. de Boer, in *Coulomb Excitation,* edited by K. Alder and A. Winther (Academic, New York, 1966), p. 303.

[21]E. N. Shurshikov, Nucl. Data Sheets **47**, 433 (1986).

[22]V. S. Shirley, Nucl. Data Sheets **53**, 223 (1988).

[23]T. J. Humanic, J. X. Saladin, J. G. Alessi, and A. Hussein, Phys. Rev. C **27**, 550 (1983).

[24]*Table of Isotopes,* 7th ed., edited by C. M. Lederer and V. S. Shirley (Wiley, London, 1978) Append. VII.

[25]G. Seiler-Clark, D. Pelte, H. Emling, A. Bacanda, H. Grein, E. Grose, R. Kulsea, D. Schwalm, H. J. Wollersheim, M. Hass, G. J. Kumbartzki, and K.-M. Speidel, Nucl. Phys. **A415**, 215 (1984).

[26]H. Andrews, O. Hausser, D. Ward, P. Taras, R. Nicole, J. Keinonen, P. Skensved, and B. Haas, Nucl. Phys. **A383**, 509 (1982).

[27]A. E. Stuchbery, H. H. Bolotin, A. P. Byrne, C. E. Doran, and G. J. Lampard, Z. Phys. A **330**, 131 (1988), and references cited therein.

[28]M. Diebel, A. N. Mantri, and U. Mosel, Nucl. Phys. **A345**, 72 (1980).

[29]Y. S. Chen, P. B. Semmes, and G. A. Leander, Phys. Rev. C **34**, 1935 (1986).

[30]G. A. Leander (private communication).

[31]S. Kuyucak, A. Faessler, and M. Wakai, Nucl. Phys. **A420**, 83 (1984), and references cited therein.